

Effect of a Percutaneous Screw Guide on Screw Placement for Posterior Talar Fractures

Ann. Ital. Chir., 2024 95, 4: 648–656
<https://doi.org/10.62713/aic.3382>

Hua Wang¹, Jichong Ying², Jianlei Liu², Tianming Yu², Dichao Huang²

¹Department of Medical Imaging, Ningbo No.6 Hospital, 315000 Ningbo, Zhejiang, China

²Department of Orthopedics, Ningbo No.6 Hospital, 315000 Ningbo, Zhejiang, China

AIM: This study aimed to evaluate the hypothesis that the utilization of percutaneous screw guides enhances the precision of screw placement in the surgical fixation of talar fractures.

METHODS: Computed tomography (CT) scans of ankle joints were obtained from 40 healthy adults and 10 cadaveric specimens between April 2019 and August 2020 at Ningbo No. 6 Hospital. The acquired CT data were imported into Materialise Interactive Medical Image Control System (MIMICS) software for processing. Three-dimensional (3D) digital models of the ankle joints were reconstructed, and relevant anatomical parameters were measured. A percutaneous screw guide (PSG) was designed and fabricated to facilitate accurate screw placement in the posterior talar process. Ten eligible cadaveric ankle joints were selected for further analysis and their 3D models were reconstructed using the MIMICS software. Screw trajectory parameters were then measured and analyzed based on these cadaveric models, forming the model group for comparative analyses. Ten cadaveric specimens were utilized in this study, equally divided into two groups: a guider group (n = 5) and a free-hand group (n = 5). In the guider group, talar posterior process screws were inserted using percutaneous screw guidance. In the free-hand group, screws were inserted into the talar posterior process without guidance. Post-operative CT scans were performed on all specimens. The following parameters were quantitatively compared between the two groups: screw trajectories, entry point distances in specimens with preselected screws, entry point distance trajectories in the 3D model, operation time, frequency of fluoroscopic imaging, and number of drilling attempts.

RESULTS: Following the generation of the 3D models from 10 cadavers, a virtual screw was digitally inserted into each model. In the model group, the preselected screw trajectory was oriented towards the medial aspect of the talar neck base, with a cephalad inclination angle (CIA) of $3.1^\circ \pm 1.5^\circ$ in the transverse plane and a medial diverge angle (MDA) of $12.0^\circ \pm 1.4^\circ$ in the coronal plane. The CIA and MDA of the screw trajectory in the guider group were $2.1^\circ \pm 1.7^\circ$ and $11.2^\circ \pm 1.6^\circ$, respectively, whereas the CIA and MDA in the free-hand group were $6.0^\circ \pm 2.2^\circ$ and $18.8^\circ \pm 1.6^\circ$, respectively. Statistical analysis revealed significant differences in both CIA and MDA between the two groups ($p < 0.05$). Furthermore, the guider group yielded superior outcomes in terms of entry point distance, operation time, fluoroscopic exposure time, and number of drilling attempts compared to the free-hand group ($p < 0.05$).

CONCLUSIONS: Percutaneous screw guidance can improve the accuracy and safety of the posterior process of the talar screws, which can be feasible for percutaneous fixation. Further studies are required to confirm the efficacy and clinical outcomes of percutaneous screw guidance.

Keywords: posterior process of talar fracture; percutaneous screw guide (PSG); cadaveric study; 3D model analysis

Introduction

Posterior talar fractures are rare and tend to be misdiagnosed on standard radiography [1]. Patients may experience persistent pain, bone nonunion, and tarsal tunnel syndrome due to missed diagnoses or inappropriate treatment [2, 3]. Moreover, the posterior process of the talar is a pivotal anatomical structure involving both the posterior facet of the subtalar and posterior ankle. Consequently, joint misalignment and post-traumatic arthritis may occur, even with minimal displacement of the fracture fragment [4].

Orthopedic surgeons use open reduction and internal fixation (ORIF) to treat posterior talar fractures. At the final follow-up examination, the patient presented bone union of the fracture. Similarly, Chen *et al.* [5] reported that ORIF utilizing miniscrew fixation can achieve satisfactory clinical outcomes in patients with fractures of the posterior talar process.

ORIF has been demonstrated to be both feasible and safe [5]. However, the procedure presents significant challenges due to the complex anatomical structure of the region, which encompasses the ankle subtalar joint and the flexor hallucis longus tendon. Consequently, ORIF is considered a technically demanding surgical approach with a prolonged learning curve for surgeons. Multiple studies have reported potential complications associated with

Correspondence to: Dichao Huang, Department of Orthopedics, Ningbo No.6 Hospital, 315000 Ningbo, Zhejiang, China (e-mail: hsdichao-huang@163.com).

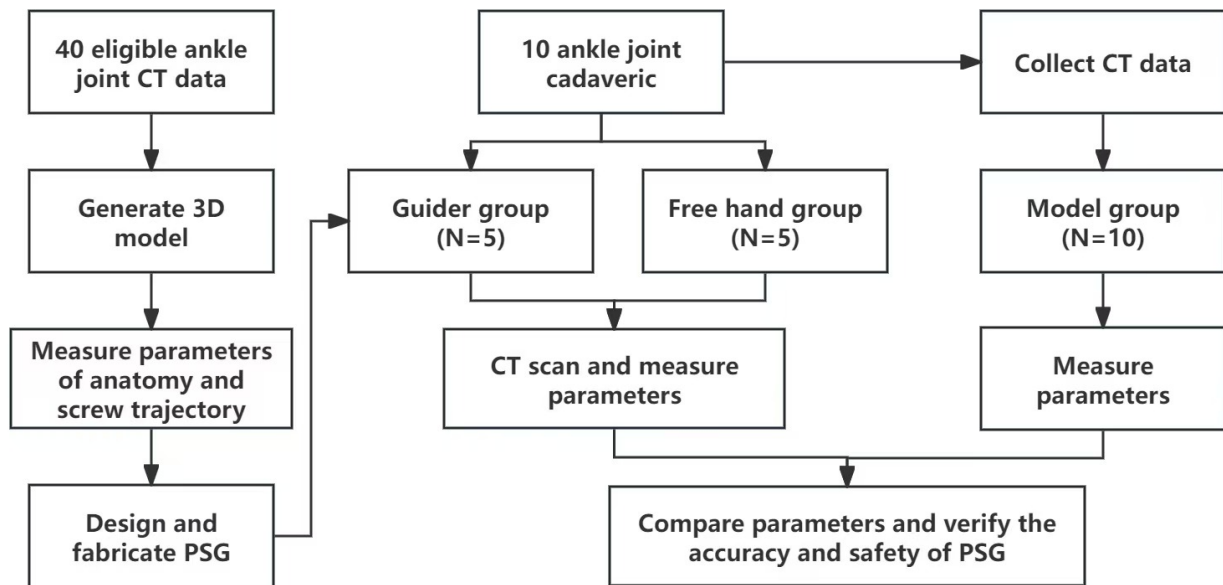


Fig. 1. Flow diagram of this study. 3D, three-dimensional; CT, computed tomography; PSG, percutaneous screw guide.

ORIF, including chronic pain, wound infection, nonunion, and post-traumatic osteoarthritis [4, 6].

Recent studies have investigated the safe zone for screw trajectory and minimally invasive fixation techniques for the posterior process of talus fractures. These techniques can shorten operation time and reduce surgical complications [7, 8]. Moreover, percutaneous fixation is a feasible alternative for patients with multiple comorbidities and high perioperative risk. However, manual placement of percutaneous screws requires increased operation time and intraoperative X-ray examinations. Many findings have reported that three-dimensional (3D) printing and robot-assisted navigation systems provide greater accuracy for preselected screw trajectories [9]. However, some studies have noted that while navigation systems can facilitate screw fixation and reduce the failure rate of screw insertion, the high cost of equipment and complex surgical procedures limit their widespread clinical adoption [10, 11, 12]. Consequently, the design and application of percutaneous screw guides for ankle joints remain under development.

Therefore, percutaneous screw guidance, a special tool that may enhance the accuracy and safety of fixation, is necessary in percutaneous techniques. We developed a percutaneous screw guide (PSG) based on the anatomy of the ankle joint and screw parameters for this fracture type. To evaluate the PSG, we performed guider-assisted percutaneous screw fixation in 10 cadavers and compared the results to those obtained using a minimally invasive technique described in our previous study [8].

Materials and Methods

In this study, computed tomography (CT) data from 40 healthy adults were collected between April 2019 and August 2020 at Ningbo No. 6 Hospital. Additionally, 10 eligible cadaveric specimens were obtained from the Medical School of Ningbo University. Informed consent was obtained from all participants, and their data were stored and used for research anonymously. This study was approved by the Institutional Review Board and Ethics Committee of Ningbo No. 6 Hospital (Ethics Committee Reference Number: 2024-21(L)). The inclusion criteria were as follows: (1) age between 20 and 55, (2) participants who consented to enroll in the study. The exclusion criteria were as follows: (1) age <20 years or >55 years, (2) history of ankle joint surgery, and (3) presence of trauma, tumor, or rheumatic arthritis.

Digital Measurement and PSG Design

Following analysis, a cohort of 40 eligible adult participants was enrolled in this study, comprising 25 males and 15 females, with an average age of 37.3 ± 13.5 years. The study protocol is illustrated in Fig. 1 (Diagram created using Lark (version 5.23.1, Lark Technologies Pte. Ltd., Singapore)). All CT scan data were converted to the Digital Imaging and Communications in Medicine (DICOM) 3.0 format and subsequently imported into Materialise Interactive Medical Image Control System (MIMICS) 19.0 (Materialize, Leuven, Belgium), a commercially available 3D reconstruction software package. The CT data from all participants successfully generated a 3D reconstruction model of the ankle joint. After generating 3D models of the ankle joints from 40 adults and 10 cadavers using MIMICS 19.0 software, the

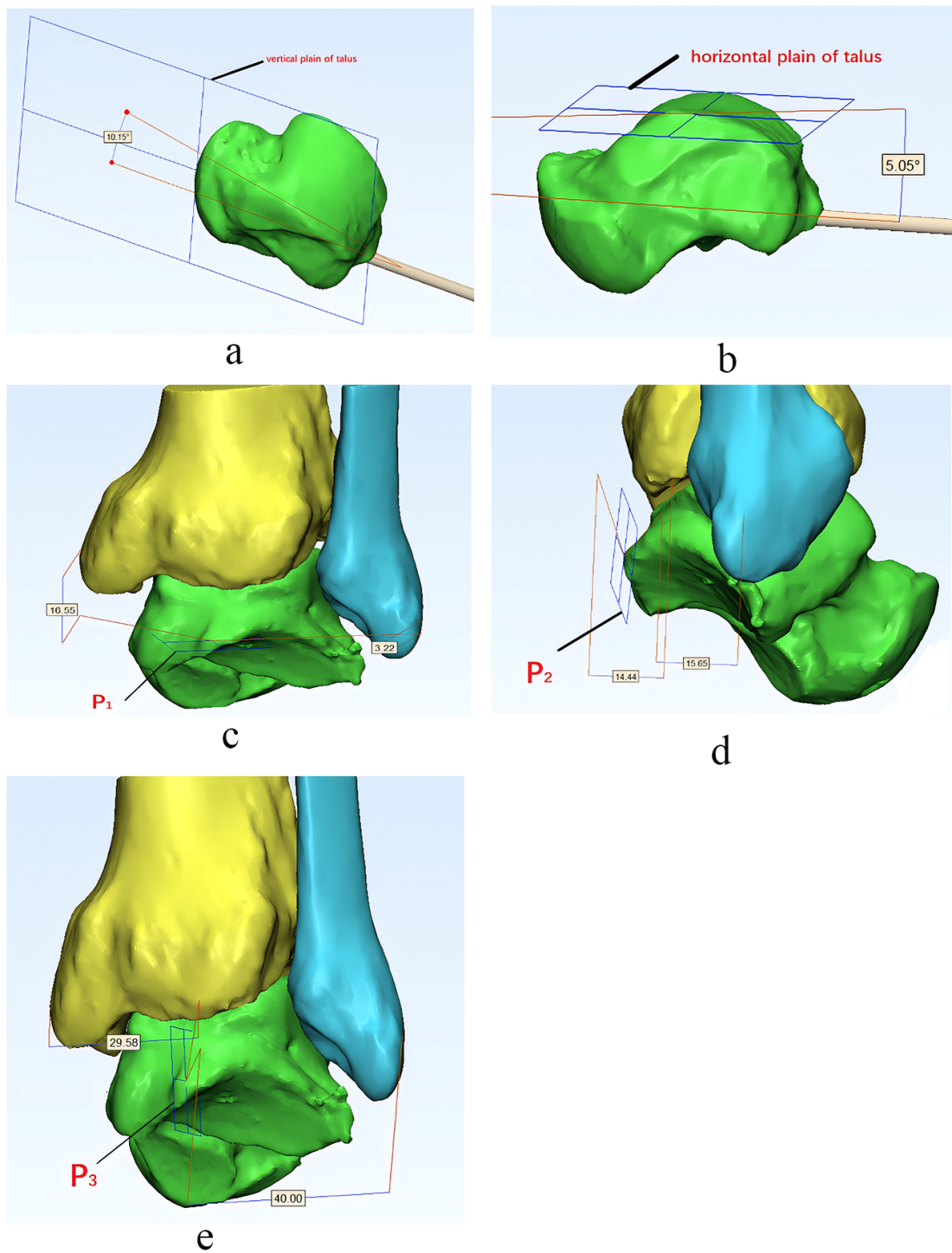


Fig. 2. The three-dimensional (3D) model of talus. (a,b) Horizontal and vertical planes of the talus were built, and then the cephalad inclination angle (CIA) and medial diverge angle (MDA) were measured between the screw and two planes. (c–e) After the horizontal plane (P₁), vertical plane (P₂) and coronal plane (P₃) of the posterior talar process were established, the vertical distance between the apex of the posterolateral process of talus and medial malleolus (AMVD), the horizontal posterior distance between the apex of the posterolateral process of talus and medial malleolus (AMHPD), the horizontal medial distance between the apex of the posterolateral process of talus and medial malleolus (AMHMD), the vertical distance between the apex of the posterolateral process of talus and lateral malleolus (ALVD), the horizontal posterior distance between the apex of the posterolateral process of talus and lateral malleolus (ALHPD), and the horizontal medial distance between the apex of the posterolateral process of talus and lateral malleolus (ALHMD) were measured.

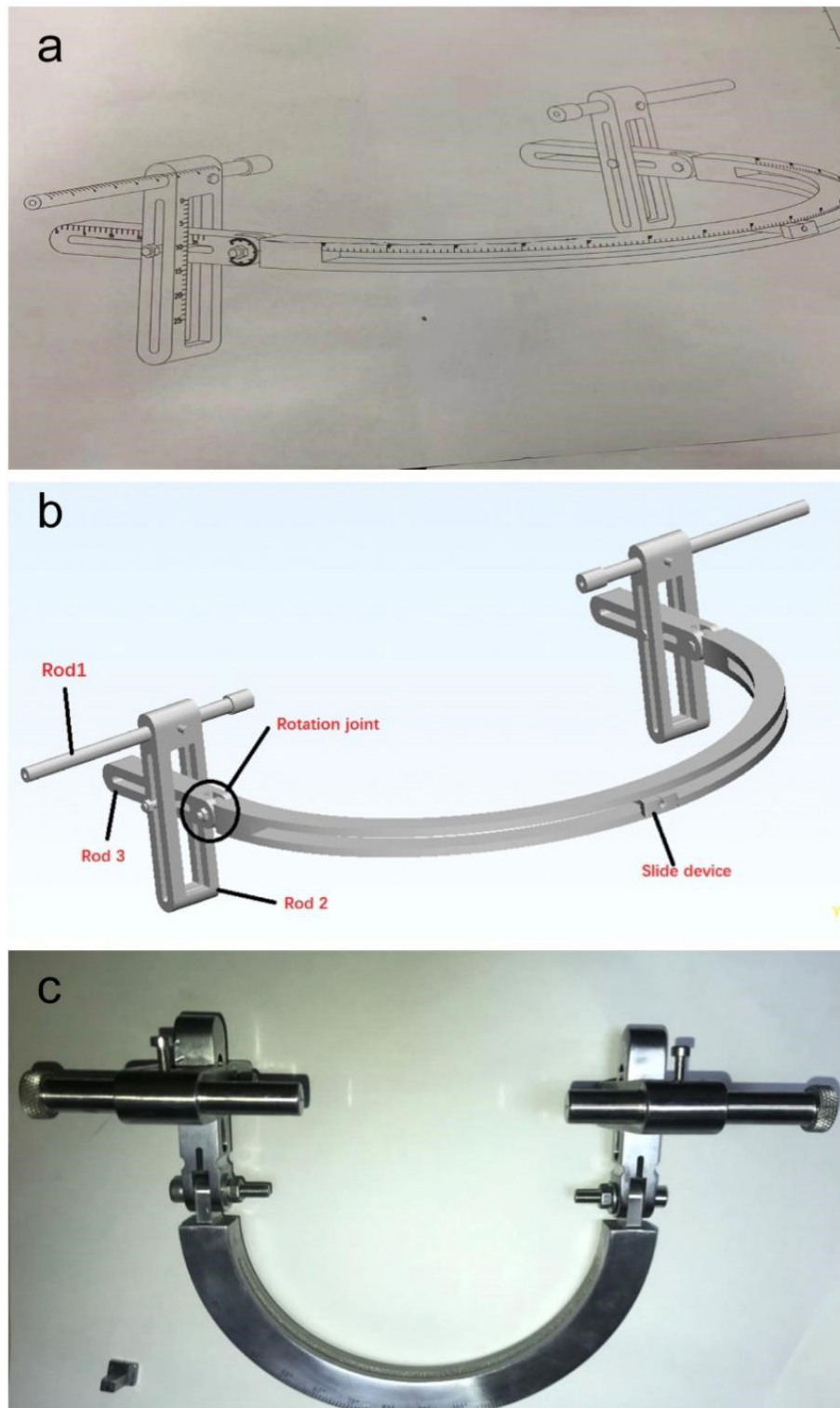


Fig. 3. Homemade percutaneous screw guide (PSG). (a) The details of the design of PSG in 3D. (b) Picture of percutaneous screw guide. The length of Rod 1, 2, and 3 could be adjusted personally, and the rotation joint and slide device can be adjusted based on the cephalad inclination angle and cephalad inclination angle. (c) Real product photo of the PSG.

horizontal and vertical planes of the talus were built according to the methodology proposed by Gutekunst *et al.* [13]. The horizontal plane (P_1), vertical plane (P_2), and coronal plane (P_3) of the posterior talar process were also established. Subsequently, all anatomical parameters (the verti-

cal distance between the apex of the posterolateral process of talus and medial malleolus (AMVD), the horizontal posterior distance between the apex of the posterolateral process of talus and medial malleolus (AMHPD), the horizontal medial distance between the apex of the posterolateral

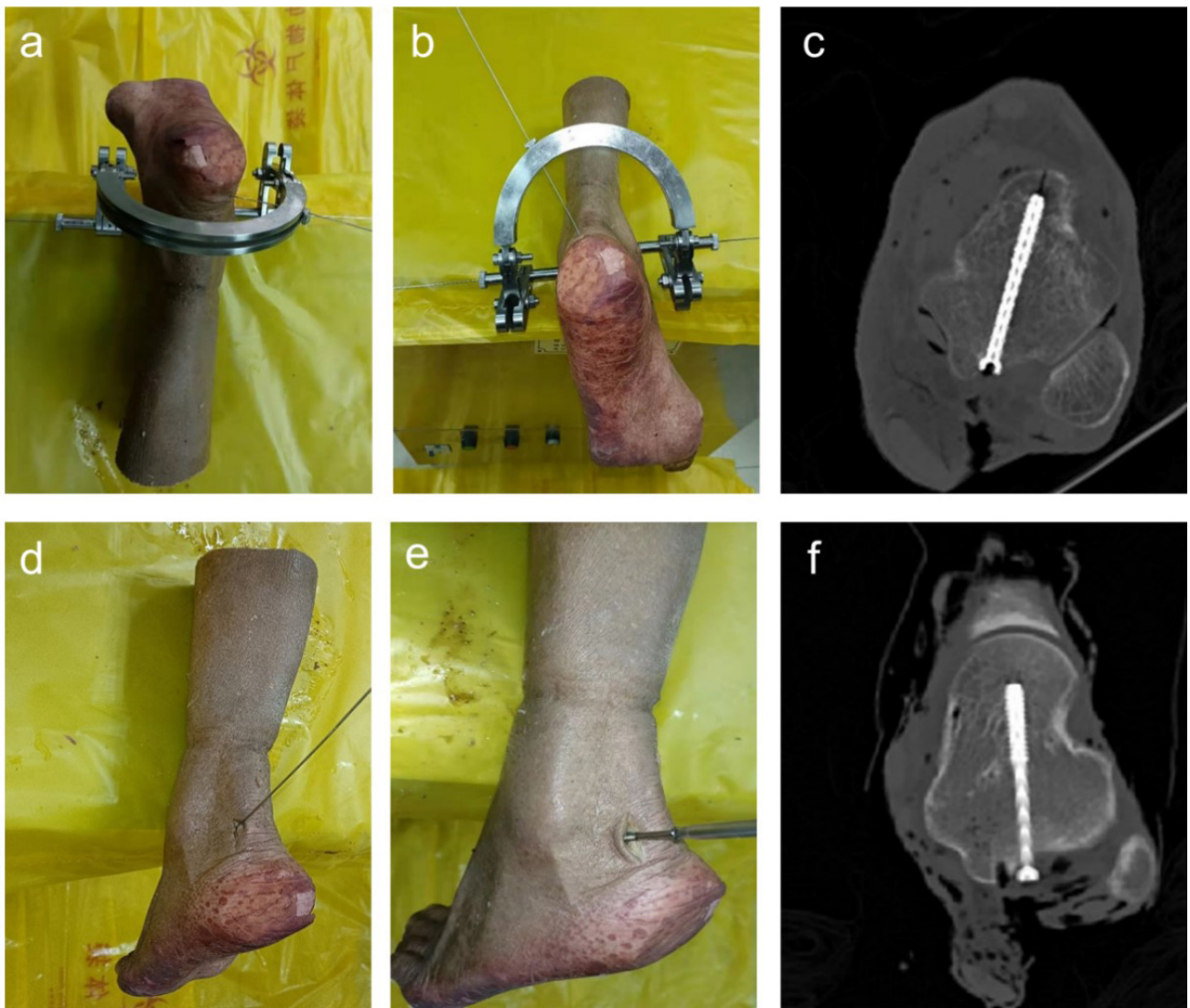


Fig. 4. Specimen simulation. (a,b) The operation procedures of percutaneous fixation with PSG in a cadaveric specimen. (c) The typical computed tomography (CT) data of the PSG group. (d,e) The operation procedures of percutaneous fixation by free hand in a cadaveric specimen. (f) The typical CT data of the free-hand group.

process of talus and medial malleolus (AMHMD), the vertical distance between the apex of the posterolateral process of talus and lateral malleolus (ALVD), the horizontal posterior distance between the apex of the posterolateral process of talus and lateral malleolus (ALHPD), and the horizontal medial distance between the apex of the posterolateral process of talus and lateral malleolus (ALHMD)) and preselected trajectory measurements [cephalad inclination angle (CIA) and medial diverge angle (MDA)] were obtained using MIMICS 19.0 (Fig. 2). Based on these anatomical parameters and preselected trajectory, PSG was designed for percutaneous screw fixation of the posterior talar process (Fig. 3). The accuracy and safety of PSG were evaluated through cadaveric simulation studies.

Table 1. The parameters of anatomy and preselected trajectory in 3D models.

Parameters	3D models
Models number	50
AMVD (mm)	11.2 ± 0.8
AMHPD (mm)	19.4 ± 1.4
AMHMD (mm)	27.8 ± 1.1
ALVD (mm)	3.7 ± 0.4
ALHPD (mm)	15.3 ± 1.3
ALHMD (mm)	30.1 ± 1.4

Specimen Simulation

In the guider group, percutaneous screw fixation assisted by PSG was performed on five dry cadavers. The details of the operation were as follows: first, a minimal incision was made between the medial malleolus and the Achilles ten-

Table 2. Comparison of operation outcomes between the guider group and the free-hand group.

Parameters	Guider group	Free hand group	<i>p</i> -value
Ankle number	5	5	
Entry point distance (mm)	0.7 ± 0.3	1.7 ± 0.5	0.01
Operation time (min)	24.0 ± 5.2	39.2 ± 5.8	0.03
Operation fluoroscopy (times)	3.8 ± 1.3	7.2 ± 1.3	0.03
Drilling attempts (times)	2.8 ± 0.8	5.6 ± 0.5	<0.001

Entry point distance, the length between the screw entry point and the apex of the posterior talus process.

Table 3. Comparison of screw trajectory among the guider, free-hand and model groups.

	Guider group	Free-hand group	Model group	<i>p</i> ₁ -value	<i>p</i> ₂ -value	<i>p</i> ₃ -value
Ankle number	5	5	10			
CIA (°)	2.1° ± 1.7°	6.0° ± 2.2°	3.1° ± 1.5°	0.25	0.01	0.005
MDA (°)	11.2° ± 1.6°	18.8° ± 1.6°	12.0° ± 1.4°	0.32	<0.001	<0.001

*p*₁, Independent T- compared between the guider and model groups; *p*₂, Independent T- compared between the free-hand group and the model group; *p*₃, Independent T- compare between the Guider and Free hand groups; CIA, cephalad inclination angle; MDA, medial diverge angle.

don, exposing and protecting the posterior tibial artery and nerve. The posterior process of the talus was then exposed. Subsequently, the posterior articular guide (PAG) was adjusted according to anatomical parameters, CIA, and MDA. Specifically, two Rod 1s were attached at the surfaces of the medial and lateral malleolus and adjusted according to the AMHMD and ALHMD, respectively. Subsequently, two Rod 2s were adjusted according to AMVD and ALVD, respectively. Following this, two Rod 3s were adjusted according to AMHPD and ALHPD. Finally, the rotation joint and slide device were adjusted based on the cephalad inclination angle. Next, K-wires were inserted into the processus posterior of the talus via the slide device, and a bone cannula was drilled using an electric drill. The PSG was then removed, and the correct placement of the wires was verified using C-arm fluoroscopy. Finally, a 3.0 mm cannulated screw (20173466187, Synthes Inc., Shanghai, China) was inserted over the K-wires (Fig. 4).

In the free-hand group, the surgical technique was modified as follows: a minimal incision was made in the interval between the medial malleolus and the Achilles tendon. Using the free-hand technique, a K-wire was inserted in a post-anterior direction from the apical part of the posterolateral process of the talus. The position of the K-wire was then verified with fluoroscopy. Subsequently, a 3.0 mm cannulated screw was inserted over the K-wire.

All specimens were scanned with CT preoperatively and postoperatively.

Outcome Measurement

After generating 3D models from preoperative and postoperative CT scans of the specimens, CIA and MDA were measured using the aforementioned method. Additionally, the entry point distance, defined as the length between the screw entry point and the apex of the posterior talar pro-

cess, was quantified. Intraoperative data, including operation duration, fluoroscopy exposure time, and the number of drilling attempts, were recorded during each operation.

Statistical Analysis

All results were presented as mean ± standard deviation (SD). The cephalad inclination angle and medial diverge angle of the two groups with 3D models were analyzed using an independent samples *t*-test in SPSS version 21.0 (IBM Corp., Chicago, IL, USA). Independent samples *t*-test was also used to compare cephalad inclination angle, medial diverge angle, entry point distance, operation times, operation fluoroscopy time, and drilling attempts between the guider and free-hand groups. Statistical significance was set at *p* < 0.05 for all analyses.

Results

The CT images of 40 healthy adults and 10 cadavers were successfully converted into 3D models, enabling the measurement of anatomical parameters (Table 1). The AMVD, AMHPD, AMHMD, ALVD, ALHPD, and ALHMD of the ankle joint were 11.2 ± 0.8 mm, 19.4 ± 1.4 mm, 27.8 ± 1.1 mm, 3.7 ± 0.4 mm, 15.3 ± 1.3 mm, and 30.1 ± 1.4 mm, respectively. The preselected screw trajectory was oriented towards the medial aspect of the talar neck base, with a CIA of 3.1° ± 1.5° in the transverse plane and an MDA of 12.0° ± 1.4° in the coronal plane. Subsequently, a percutaneous screw guide was designed with rods that can be adjusted according to AMVD, AMHPD, AMHMD, ALVD, ALHPD, and ALHMD. The rotation joint and slide device were designed to be adjustable based on the CIA and MDA.

In the cadaver simulation, the guider group demonstrated significantly better outcomes compared to the free-hand group in terms of entry point distance (0.7 ± 0.3 vs 1.7 ± 0.5 mm), operation time (24.0 ± 5.2 vs 39.2 ± 5.8 min), flu-

oroscopy time (3.8 ± 1.3 vs 7.2 ± 1.3 times), and drilling attempts (2.8 ± 0.8 vs 5.6 ± 0.5 times) ($p < 0.05$ for all comparisons) (Table 2). No statistically significant differences were observed between the guider and model groups regarding CIA and MDA ($2.1^\circ \pm 1.7^\circ$ and $11.2^\circ \pm 1.6^\circ$ vs $3.1^\circ \pm 1.5^\circ$ and $12.0^\circ \pm 1.4^\circ$, respectively) ($p > 0.05$). However, significant differences were found between the free-hand and model groups in CIA and MDA ($6.0^\circ \pm 2.2^\circ$ and $18.8^\circ \pm 1.6^\circ$ vs $3.1^\circ \pm 1.5^\circ$ and $12.0^\circ \pm 1.4^\circ$, respectively) ($p < 0.05$). The screw trajectory outcomes are presented in Table 3.

Discussion

Cedell [14] first described a series of posteromedial process fractures of the talus, proposing that these fractures were caused by talotibial ligament avulsion. Fractures of the posterior talar process are rare and frequently misdiagnosed, potentially leading to persistent pain, bone nonunion, and osteoarthritis without appropriate treatment [15]. Standard anteroposterior, ankle mortise and lateral X-ray radiography are often insufficient for accurate diagnosis. While Ebraheim *et al.* [16] reported that oblique view (45° and 70° of external rotation) may improve diagnostic accuracy compared to conventional radiography, CT scans remain superior for evaluating fragment size, measuring displacement, and guiding treatment decisions [17].

Regarding the treatment of these fractures, orthopedic surgeons opt for surgical intervention in patients with posterior talar fractures. Surgery can enhance ankle functional recovery, improve the quality of daily life, and reduce the risk of complications. Swords *et al.* [18] reported that 10 patients with posterior medial talar fractures underwent open reduction and internal fixation (ORIF), and none experienced symptoms related to the flexor hallucis longus or bone nonunion. Currently, ORIF is the most commonly employed surgical method due to its ability to facilitate the reduction of bone fragments. However, ORIF may require extended operative time and involve significant blood loss, making it less suitable for patients with higher perioperative risk. Even though our group reported the design of the screw trajectory using a 3D model preoperatively and used a minimally invasive approach, intraoperative adjustment of the K-wire direction is still unavoidable. Recent advancements in robotic and computer-assisted navigation systems have garnered significant interest, with studies demonstrating their capacity to achieve higher entry point accuracy and optimal screw distribution. However, the clinical practice of these technologies is constrained by several limitations, including increased radiation exposure, complicated installation, and high costs [19]. Consequently, there is a need for the development of a screw guide to enhance the accuracy of screw placement.

This study investigated the anatomical parameters of the ankle joint and designed a special percutaneous screw guide (PSG) with adjustable functional elements. A total of 10

cadaveric ankle joint specimens were utilized, with or without PSG application. The efficacy of PSG was evaluated in terms of screw placement accuracy, operation time, and fluoroscopy duration. The guider group exhibited significantly improved CIA and MDA of screw trajectories compared to the free-hand group. No statistically significant differences in CIA and MDA were observed between the guider and model groups, whereas the free-hand group showed inferior outcomes in these measures. Similarly, the guider group exhibited shorter fluoroscopy times and required fewer drilling attempts compared to the free-hand group. Additionally, the entry point distance was significantly reduced with the use of PSG. This improvement is attributed to the precision of PSG, which allows for the projection of screw insertion for each individual based on preoperative radiological outcomes. The accuracy of the entry point and screw direction was enhanced through modifications to the PSG design. Specifically, the scale of rods, rotation joint, and slide device were implemented to precisely determine the entry point, CIA, and MDA, respectively. Zhu *et al.* [20] developed a screw guide for femoral neck sections and compared radiological outcomes between guider-assisted and conventional techniques using 10 cadaveric specimens. Their findings demonstrated improved accuracy in optimal screw positioning and enhanced operative outcomes with the utilization of the screw guider [20]. Luo *et al.* [21] reported similar results for pedicle screw placement assisted by the pedicle guide technique. The accuracy rate of pedicle screw insertion and surgical outcomes, including mean time per screw placement and screw-related complications, were significantly improved in the pedicle group compared to the control group [21]. This study presents several limitations. First, the investigation was constrained by a limited sample size of cadaveric specimens, which may impact the generalizability of the findings. Second, the research protocol did not include the generation of models for the posterior tibial artery, flexor hallucis longus tendon, or plantar nerve around the talus. Therefore, the positions of these pivotal anatomical structures were not considered in the analysis. However, this may not significantly influence the results, as these structures are mostly located medially. Third, we used an intact talus to simulate the anatomic reduction of talar posterolateral process fractures. Percutaneous fixation may be unsuitable for comminuted or unstable fractures, as open reduction is often necessary to prevent bone union. Studies including more cadaveric samples and prospective clinical cases with increased patient cohorts, are necessary to validate the precision and safety of percutaneous fixation with PSG.

Conclusions

Fractures of the posterior process of the talus are uncommon and often misdiagnosed or diagnosed late in clinical practice. Minimally invasive techniques allow for easier access to fracture fragment reduction and require less operative time compared to ORIF. However, these minimally invasive methods may not ensure the accuracy of screw trajectory, often necessitating repeated intraoperative fluoroscopy and multiple drilling attempts. This study provides preliminary data on the use of percutaneous fixation with PSG for posterior talar fractures. PSG can enhance the accuracy and safety of percutaneous fixation, presenting an alternative method for robot- and computer-assisted navigation systems.

Availability of Data and Materials

The datasets used during the current study are available from the corresponding author on reasonable request.

Author Contributions

HW and DH conceived and designed the research study. JY, JL, and TY performed the research and collected the data. HW and DH provided oversight and guidance throughout the project. JY analyzed the data. HW drafted the manuscript, and all authors revised it critically for important intellectual content. All authors read and approved the final manuscript. All authors have participated sufficiently in the work and agreed to be accountable for all aspects of the work.

Ethics Approval and Consent to Participate

This study was conducted in accordance with the ethical standards of the institutional and national research committee and the Helsinki declaration and its later amendments or comparable ethical standards. The use of cadaveric specimens and human CT scan data was approved by the Institutional Review Board and Ethics Committee of Ningbo No. 6 Hospital (Ethics Committee Reference Number: 2024-21(L)). Written informed consent was obtained from all participants or their legal guardians for the use of their CT scan data in this study. For the cadaveric specimens, consent for use in medical research and education was obtained prior to donation, in compliance with the legal and ethical requirements. 10 eligible cadaveric specimens were obtained from the Medical School of Ningbo University. The cause of death was natural death. They all donated their bodies voluntarily during their lifetime.

Acknowledgment

Not applicable.

Funding

This work was supported by Science and Technology Projects in the Field of Agriculture and Social Development

in Yinzhou District (No.2021AS0064), Ningbo Public Welfare Research Program Project in Zhejiang Province (No. 20211JCGY020058).

Conflict of Interest

The authors declare no conflict of interest.

References

- [1] Majeed H, McBride DJ. Talar process fractures: An overview and update of the literature. *EFORT Open Reviews*. 2018; 3: 85–92.
- [2] Veazey BL, Heckman JD, Galindo MJ, McGanity PL. Excision of ununited fractures of the posterior process of the talus: a treatment for chronic posterior ankle pain. *Foot & Ankle*. 1992; 13: 453–457.
- [3] Stefko RM, Laueran WC, Heckman JD. Tarsal tunnel syndrome caused by an unrecognized fracture of the posterior process of the talus (Cedell fracture). A case report. *The Journal of Bone and Joint Surgery. American Volume*. 1994; 76: 116–118.
- [4] Wijers O, Engelmann EWM, Posthuma JJ, Halm JA, Schepers T. Functional Outcome and Quality of Life After Nonoperative Treatment of Posterior Process Fractures of the Talus. *Foot & Ankle International*. 2019; 40: 1403–1407.
- [5] Chen YJ, Hsu RW, Shih HN, Huang TJ. Fracture of the entire posterior process of talus associated with subtalar dislocation: a case report. *Foot & Ankle International*. 1996; 17: 226–229.
- [6] von Winning D, Lippisch R, Pliske G, Adolf D, Walcher F, Piatek S. Surgical treatment of lateral and posterior process fractures of the talus: Mid-term results of 15 cases after 7 years. *Foot and Ankle Surgery: Official Journal of the European Society of Foot and Ankle Surgeons*. 2020; 26: 71–77.
- [7] Mao H, Wang H, Wang L, Yao L. Definition of a safe zone for screw fixation of posterior talar process fracture by 3-dimensional technology. *Medicine*. 2018; 97: e13331.
- [8] Mao H, Wang H, Zhao J, Wang L, Yao L, Wei K. Initial assessment of treatment of talar posterior process fractures with open reduction and percutaneous fixation. *Scientific Reports*. 2020; 10: 20221.
- [9] Duan SJ, Liu HS, Wu WC, Yang K, Zhang Z, Liu SD. Robot-assisted Percutaneous Cannulated Screw Fixation of Femoral Neck Fractures: Preliminary Clinical Results. *Orthopaedic Surgery*. 2019; 11: 34–41.
- [10] Chiu WK, Luk WK, Cheung LK. Three-dimensional accuracy of implant placement in a computer-assisted navigation system. *The International Journal of Oral & Maxillofacial Implants*. 2006; 21: 465–470.
- [11] Khan A, Rho K, Mao JZ, O'Connor TE, Agyei JO, Meyers JE, et al. Comparing Cortical Bone Trajectories for Pedicle Screw Insertion using Robotic Guidance and Three-Dimensional Computed Tomography Navigation. *World Neurosurgery*. 2020; 141: e625–e632.

- [12] Wang R, Zhang Z, Li Z, Qu Y. Retrosigmoid approach assisted by high-resolution computed tomography: a cost-effective technique to identify the transverse and sigmoid sinus transition. *Chinese Neurosurgical Journal*. 2020; 6: 12.
- [13] Gutekunst DJ, Liu L, Ju T, Prior FW, Sinacore DR. Reliability of clinically relevant 3D foot bone angles from quantitative computed tomography. *Journal of Foot and Ankle Research*. 2013; 6: 38.
- [14] Cedell CA. Rupture of the posterior talotibial ligament with the avulsion of a bone fragment from the talus. *Acta Orthopaedica Scandinavica*. 1974; 45: 454–461.
- [15] Engelmann EWM, Wijers O, Posthuma JJ, Schepers T. Systematic review: Diagnostics, management and outcome of fractures of the posterior process of the talus. *Injury*. 2020; 51: 2414–2420.
- [16] Ebraheim NA, Patil V, Frisch NC, Liu X. Diagnosis of medial tubercle fractures of the talar posterior process using oblique views. *Injury*. 2007; 38: 1313–1317.
- [17] Mehrpour SR, Aghamirsalim MR, Sheshvan MK, Sorbi R. Entire posterior process talus fracture: a report of two cases. *The Journal of Foot and Ankle Surgery: Official Publication of the American College of Foot and Ankle Surgeons*. 2012; 51: 326–329.
- [18] Swords M, Shank J, Benirschke S. Surgical Treatment of Posteromedial Talus Fractures: Technique Description and Results of 10 Cases. *Indian Journal of Orthopaedics*. 2018; 52: 269–275.
- [19] Passias PG, Brown AE, Alas H, Bortz CA, Pierce KE, Hassanzadeh H, et al. A cost benefit analysis of increasing surgical technology in lumbar spine fusion. *The Spine Journal: Official Journal of the North American Spine Society*. 2021; 21: 193–201.
- [20] Zhu Q, Xu B, Lv J, Yan M. Introduction of a guide based on a femoral neck section for fixation with multiple screws: a cadaveric study. *BMC Musculoskeletal Disorders*. 2018; 19: 104.
- [21] Luo M, Wang W, Yang N, Xia L. Does Three-dimensional Printing Plus Pedicle Guider Technology in Severe Congenital Scoliosis Facilitate Accurate and Efficient Pedicle Screw Placement? *Clinical Orthopaedics and Related Research*. 2019; 477: 1904–1912.

Publisher's Note: *Annali Italiani di Chirurgia* stays neutral with regard to jurisdictional claims in published maps and institutional affiliations.